Correspondence

Error-Event Characterization on Partial-Response Channels

Shirish A. Altekar, Magnus Berggren,
Bruce E. Moision, *Student Member, IEEE*,
Paul H. Siegel, *Fellow, IEEE*,
and Jack K. Wolf, *Fellow, IEEE*

***Abstract*— Two algorithms for characterization of input error events producing specified distance at the output of certain binary-input partial-response (PR) channels are presented. Lists of error events are tabulated for PR channels of interest in digital recording.**

***Index Terms*— Constrained codes, error events, intersymbol interference, magnetic recording, partial-response channels.**

I. Introduction

Consider a communication system in which a sequence $x(D)$ drawn from a finite alphabet $\mathcal{A}$ is transmitted over a channel with finite impulse response given by a polynomial $h(D) = h_0 + h_1 D + \cdots + h_\nu D^\nu$ of degree ν. The noiseless output of the channel is $y(D) = h(D)x(D)$. Let $n(D)$ be a sequence of uncorrelated zero-mean Gaussian random variables with variance σ^2. A Viterbi detector observes the noisy channel output sequence $y(D) + n(D)$ and forms the maximum-likelihood estimate $x'(D)$ of the transmitted sequence $x(D)$.

Define the input error sequence $\varepsilon_x(D) = x(D) - x'(D)$ and the output error sequence $\varepsilon_y(D) = h(D)\varepsilon_x(D)$. The performance of the system is largely dictated by input error sequences $\varepsilon_x(D)$ that result in an output with small squared Euclidean distance

$$\|\varepsilon_y(D)\|^2 = \sum_k \varepsilon_{y,k}^2.$$

By characterizing the error sequences with a small Euclidean distance, one can design codes which can eliminate them giving a performance improvement [3], [11], [10], [8], [4], [7]. For channels where $h(e^{j\omega})$ has zeros on the unit circle, the characterization is complicated by the presence of input sequences with $\|h(D)\varepsilon_x(D)\|^2 = 0$. These sequences preclude a simple tree-search for all $\varepsilon_x(D)$ with small Euclidean distance. The purpose of this note is to give two algorithms for characterizing the low distance error sequences. These algorithms are applied to binary-input partial-response (PR) channels of the form

$$h(D) = (1 - D)^m (1 + D)^n \tag{1}$$

for integers $m, n \geq 0$ which are good models for magnetic and optical recording channels.

Manuscript received October 1, 1997; revised May 1, 1998. The work of S. A. Altekar was supported by a Western Digital Fellowship. The work of B. E. Moision was supported in part by the Center for Magnetic Recording Research, University of California at San Diego, and by the University of California MICRO Project 96-124 in cooperation with GEC Plessey Semiconductors, Inc. The work of P. H. Siegel was supported in part by the University of California MICRO Project 96-124 in cooperation with GEC Plessey Semiconductors, Inc., and by NSF under Grant NCR-9612802. The work of J. K. Wolf was supported in part by NSF under Grant NCR-9405008. The material in this correspondence was presented at the IEEE International Symposium on Information Theory, Ulm, Germany, June 29–July 4, 1997.

S. A. Altekar is with DataPath Systems, Inc., Los Gatos, CA 95039 USA.
M. Berggren is with Conexant, San Diego, CA 92121-3707 USA.
B. E. Moision, P. H. Siegel, and J. K. Wolf are with the University of California at San Diego, La Jolla, CA 92093–0407 USA.

Communicated by E. Soljanin, Associate Editor for Coding Techniques.
Publisher Item Identifier S 0018-9448(99)00075-9.

II. Error State Diagram

For convenience, the following taxonomy of error sequences will be employed. A *closed error event* is a polynomial input error sequence

$$\varepsilon_x(D) = \sum_{k=k_1}^{k_2} \varepsilon_{x,k} D^i$$

where k_1 and k_2 are finite integers and $\varepsilon_{x,k_1} \neq 0$ and $\varepsilon_{x,k_2} \neq 0$. A closed error event is said to be *simple* if the condition $\varepsilon_{x,k} = \varepsilon_{x,k+1} = \cdots = \varepsilon_{x,k+\nu-1} = 0$ is not true for any integer $k_1 \leq k \leq k_2 - \nu$. Otherwise, the closed error event is said to be *compound*. An *open error event* is a right-infinite input error sequence of the form

$$\varepsilon_x(D) = \sum_{k=k_1}^{\infty} \varepsilon_{x,k} D^k$$

where infinitely many $\varepsilon_{x,k}$ are nonzero and yet the squared Euclidean distance is finite, $\|\varepsilon_y(D)\|^2 < \infty$.

Let $\mathcal{A}$ be the binary alphabet, $\mathcal{A} = \{0, 1\}$. The corresponding alphabet for the input error sequences will be $\mathcal{B} = \{-1, 0, +1\}$. At times, the characters "$-$," "0," and "$+$" will be used as shorthand for the elements of $\mathcal{B}$. Input error sequences together with their corresponding squared output error sequences can be described as paths through a labeled directed graph $\mathcal{G}$ known as an *error state diagram* [12, p. 279]. The graph $\mathcal{G}$ consists of a set of 3^ν states, a finite set of edges, and an assignment of labels $\mathcal{L}(e)$ to each edge e in $\mathcal{G}$. Each state s in $\mathcal{G}$ is denoted by a distinct block of ν symbols from $\mathcal{B}$, $s = \varepsilon_{x,k-\nu} \cdots \varepsilon_{x,k-2}\varepsilon_{x,k-1}$, representing the portion of an error sequence in the channel memory. Each edge e in $\mathcal{G}$ has an initial state $\boldsymbol{i}(e) = \varepsilon_{x,k-\nu} \cdots \varepsilon_{x,k-2}\varepsilon_{x,k-1}$ corresponding to a particular channel history and terminal state $\boldsymbol{t}(e) = \varepsilon_{x,k-\nu+1} \cdots \varepsilon_{x,k-1}\varepsilon_{x,k}$ determined by the next error input symbol $\varepsilon_{x,k}$. This edge e has an input label $\mathcal{L}_{\text{in}}(e) = \varepsilon_{x,k}$ given by the current error symbol input and an output label $\mathcal{L}_{\text{out}}(e) = \varepsilon_{y,k}^2$ given by the corresponding squared output symbol. The full edge label is given in input/output form by $\mathcal{L}(e) = \mathcal{L}_{\text{in}}(e)/\mathcal{L}_{\text{out}}(e)$. An example of an error state diagram for the channel $h(D) = (1 + D)^2$, denoted PR2, is shown in Fig. 1.

The state in the error state diagram denoted by a block of all-zero error input symbols is distinguished and called the *zero-state*. A *path* in the error state diagram $e_1 e_2 \cdots e_n$ is a finite sequence of edges e_i such that $\boldsymbol{t}(e_i) = \boldsymbol{i}(e_{i+1})$ for $1 \leq i < n$. A *cycle* is a path that starts and ends at the same state. A *simple cycle* is a cycle that does not intersect itself. A *zero-cycle* in the error state diagram is a simple cycle whose output edge labels are all zero. Let $\mathcal{Z}$ denote the set of all states that are a part of some zero-cycle in $\mathcal{G}$. For the PR2 error state diagram shown in Fig. 1, the states shaded in gray form the set $\mathcal{Z}$.

Closed error events are represented by paths which start at the zero-state on the error state diagram and end at the zero-state. Open error events start at the zero-state and end in some zero-cycle other than the self-loop at the zero-state.

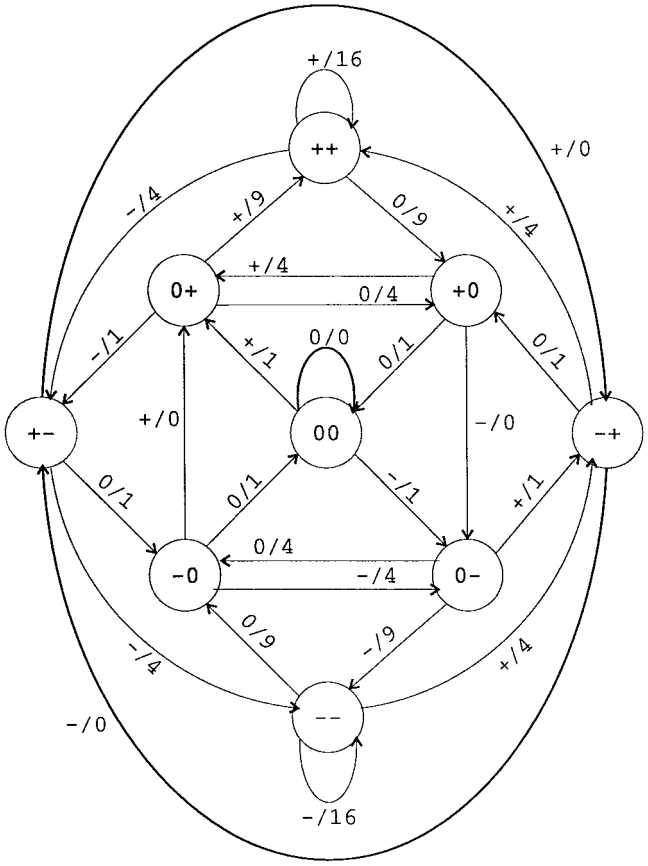

Fig. 1. Error state diagram for PR2 channel, $h(D) = (1 + D)^2$.

Error state diagrams for the linear channels considered here contain at least one zero-cycle, namely, the self-loop at the zero-state. PR channels of the form considered in this note have other zero-cycles in their error state diagrams. These stem from the presence of spectral nulls in the frequency response $h(e^{j\omega})$ at DC ($\omega = 0$) and at Nyquist ($\omega = \pi$). Associated with every zero-cycle is a periodic bi-infinite input error sequence $\varepsilon_x(D)$, known as the *null error sequence*, with the property that

$$\|h(D)\varepsilon_x(D)\|^2 = 0. \tag{2}$$

The null error sequence is obtained by reading the input edge labels on a bi-infinite walk along the zero-cycle. The sequence of states for a zero-cycle can be retrieved by sliding a window of length ν along its null error sequence.

Let $(\varepsilon_{x,1}, \varepsilon_{x,2}, \cdots, \varepsilon_{x,k})^\infty$ represent an infinite periodic sequence of input error symbols with periodic pattern given by the string within the brackets $(\cdot)$. Then the following lemma characterizes null error sequences for PR channels of the form given by (1).

Lemma 1: Let $h(D) = (1 - D)^m(1 + D)^n$. a) If $m > 0$ and $n = 0$ then the null error sequences are $(0)^\infty, (+)^\infty$ and $(-)^\infty$. b) If $m = 0$ and $n > 0$ then the null error sequences are $(0)^\infty, (+-)^\infty$ and $(-+)^\infty$. c) If $m > 0$ and $n > 0$ then the null error sequences are $(0)^\infty, (+)^\infty, (-)^\infty, (+-)^\infty, (-+)^\infty, (+0)^\infty, (0+)^\infty, (-0)^\infty$, and $(0-)^\infty$.

Proof: A proof of part c) of the lemma is given. The other parts have a similar proof. By Parseval's relation, any input error sequence $\varepsilon_x(D)$ that satisfies (2) must also satisfy

$$\int_{2\pi} |h(e^{j\omega})\varepsilon_x(e^{j\omega})|^2 \, d\omega = 0. \tag{3}$$

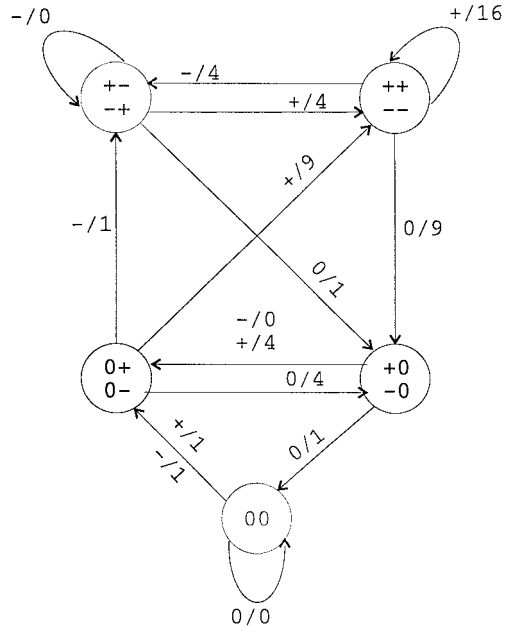

Fig. 2. Reduced error state diagram for the PR2 channel, $h(D) = (1+D)^2$.

Thus $\varepsilon_x(e^{j\omega})$ has all of its mass concentrated at the nulls of $h(e^{j\omega})$ at $\omega = k\pi$, $k \in \mathbb{Z}$, and must be of the form

$$\varepsilon_x(e^{j\omega}) = \sum_{r=-\infty}^{\infty} 2\pi a_0 \delta(\omega + 2\pi r) + 2\pi a_1 \delta(\omega - \pi + 2\pi r).$$

Therefore, by the Fourier inversion formula

$$\varepsilon_{x,n} = \frac{1}{2\pi} \int_{2\pi} \varepsilon_x(e^{j\omega}) \, d\omega = a_0 + a_1 e^{jn\pi}. \tag{4}$$

Given that $\varepsilon_{x,n} \in \mathcal{B}$, the only possible values for the pair (a_0, a_1) are $(0,0)$, $\pm(\frac{1}{2}, \pm\frac{1}{2})$, $(0, \pm 1)$, and $(\pm 1, 0)$. These values result in the null error sequences of part c) of the lemma. □

A. Reduced Error State Diagram

A new graph $\mathcal{G}'$ can be produced from $\mathcal{G}$ as follows. The states of $\mathcal{G}'$ are the states of $\mathcal{G}$. The edges of $\mathcal{G}'$ are the edges of $\mathcal{G}$ with input labels modified as follows. If e is an edge of $\mathcal{G}'$ with $\boldsymbol{i}(e) = \varepsilon_{x,k-\nu} \cdots \varepsilon_{x,k-2}\varepsilon_{x,k-1}$ and $\boldsymbol{t}(e) = \varepsilon_{x,k-\nu+1} \cdots \varepsilon_{x,k-1}\varepsilon_{x,k}$ such that $\boldsymbol{i}(e)$ is not the zero-state, it has an input label given by

$$\mathcal{L}'_{\text{in}}(e) = \varepsilon_{x,k} \cdot \varepsilon_{x,j^*} \tag{5}$$

where

$$j^* = \max\{j | \varepsilon_{x,j} \neq 0, k - \nu \leq j < k\}$$

and $\cdot$ denotes multiplication. The edge has a corresponding output label given by $\mathcal{L}'_{\text{out}}(e) = \varepsilon^2_{y,k}$. The full edge label in input/output form is given by $\mathcal{L}'(e) = \mathcal{L}'_{\text{in}}(e)/\mathcal{L}'_{\text{out}}(e)$. The edge labels with $\boldsymbol{i}(e) = 0 \cdots 0$, the zero-state, are unchanged from their representation in $\mathcal{G}$. The graph $\mathcal{G}'$ represents all input error sequences together with their squared distance in a form of *differential notation*. The main advantage of the differential notation is that $\mathcal{G}'$ contains *equivalent states* which can be merged. Two states in $\mathcal{G}'$ are equivalent if the collection of labels of paths starting at each of the states, denoted the *follower sets*, are equal. It can be shown that the two states of $\mathcal{G}'$, $s = \varepsilon_{x,k-\nu} \cdots \varepsilon_{x,k-2}\varepsilon_{x,k-1}$ and $-s = -\varepsilon_{x,k-\nu} \cdots -\varepsilon_{x,k-2} - \varepsilon_{x,k-1}$ are equivalent by using a state minimization algorithm. By merging all of the equivalent states of $\mathcal{G}'$ one obtains a new graph $\mathcal{H}$, known as a *reduced error state diagram* [12, p. 281], [9] which has $\frac{1}{2}(3^\nu - 1) + 1$ states. Fig. 2 shows the reduced error state diagram for the PR2 channel.

```
Search( state s, squared distance d^2, depth j )
If d^2 ≤ d^2_max
   If s ∈ Z
   {
      If d^2 > 0
         Print d^2 and families of error fragments
               with initial part π[1], π[2], ···, π[j];
   }
   Else
      For each edge e leaving state s
      {
          π[j] ← e;
          Search(t(e), d^2 + L_out(e), j + 1);
      }
```

Fig. 3. Pseudocode for depth-first search.

The reduced error state diagram still contains zero-cycles, with some pairs of period-2 cycles mapped into period-1 cycles. The search algorithms presented are independent of the labeled graph used to describe the error events. The algorithm presented in Section III-A will refer to the graph $\mathcal{G}$ while the algorithm in Section III-B will refer to the graph $\mathcal{H}$.

III. Search Algorithms

A. Modified Depth-First Search Algorithm

A simple depth-first search of the error state diagram can be used to find all open and closed error events of up to a specified maximum squared distance. The only complication is the presence of zero-cycles in the error state diagram. There are many ways in which this search can be done [2], [1]. A two-stage search is described here.

A path $e_1, e_2, \cdots, e_k, e_{k+1}, \cdots, e_n$ in the error state diagram is called an *error fragment* if

$$\sum_{i=1}^{n} \mathcal{L}_{\text{out}}(e_i) > 0, \boldsymbol{i}(e_1) \in \mathcal{Z},$$

$\boldsymbol{i}(e_i) \in \mathcal{Z}$, and there is an integer k such that $\boldsymbol{t}(e_i) \in \mathcal{Z}$ for $k \le i \le n$ and $\boldsymbol{t}(e_i) \notin \mathcal{Z}$ for $1 < i < k$. In other words, an error fragment is a path that accumulates positive squared distance, begins at a state in $\mathcal{Z}$, and ends on a zero-cycle without having visited any other zero-cycle. It is convenient to group families of error fragments which start at a common state and share the same sequence of initial edges, but differ in the number of edges on the ending zero-cycle. By Lemma 1, zero-cycles for the PR channels of (1) are either of period 1 or of period 2. A family of error fragments that end in the period-1 zero-cycle e_{k+1} are represented by the string

$$\mathcal{L}_{\text{in}}(e_1)\mathcal{L}_{\text{in}}(e_2)\cdots\mathcal{L}_{\text{in}}(e_k)(\mathcal{L}_{\text{in}}(e_{k+1}))$$

where the brackets $(\cdot)$ around a substring of input error symbols are used to represent repetition of that substring zero or more times. Families of error fragments which end in the period-2 zero-cycle $e_{k+1}e_{k+2}$ are represented by the two strings

$$\mathcal{L}_{\text{in}}(e_1)\mathcal{L}_{\text{in}}(e_2)\cdots\mathcal{L}_{\text{in}}(e_k)(\mathcal{L}_{\text{in}}(e_{k+1})\mathcal{L}_{\text{in}}(e_{k+2}))$$

and

$$\mathcal{L}_{\text{in}}(e_1)\mathcal{L}_{\text{in}}(e_2)\cdots\mathcal{L}_{\text{in}}(e_k)(\mathcal{L}_{\text{in}}(e_{k+1})\mathcal{L}_{\text{in}}(e_{k+2}))\mathcal{L}_{\text{in}}(e_{k+1})$$

which correspond to the two possible ending phases for the zero-cycle. In this representation, it is assumed that the initial state $\boldsymbol{i}(e_1)$ is known.

The first part of the search determines all error fragments that acquire squared distance no greater than $d^2_{\max}$. This is accomplished by a depth-first search starting from each state in $\mathcal{Z}$. The depth-first search backtracks when a state in $\mathcal{Z}$ is reached, in which case it also prints out families of error fragments corresponding to the search path, or when the maximum distance $d^2_{\max}$ has been accumulated. A recursive subroutine for this search is described via pseudocode in Fig. 3. The subroutine assumes that global storage for the path $\pi[i]$ is available, and some representation of the underlying graph $\mathcal{G}$ has been defined. The subroutine is invoked using Search$(s, 0, 0)$ for each $s \in \mathcal{Z}$.

The second part of the search constructs a graph $\mathcal{F}$ whose vertices are the states in $\mathcal{Z}$. An edge e is present in $\mathcal{F}$ if there is a family of error fragments in $\mathcal{G}$ which start at $\boldsymbol{i}(e)$ and end at $\boldsymbol{t}(e)$. The input label for the edge is the string of input error symbols representing this family, and the output label is the squared distance accumulated by these error fragments. A depth-first search of $\mathcal{F}$ starting at the zero-state, similar to that of Fig. 3, can be used to determine the lists of closed and open error events. Such a graph $\mathcal{F}$ for the PR2 channel, $h(D) = (1 + D)^2$, is given in Fig. 4. All error fragments which acquire squared distance no greater than 8 are shown.

B. Local Higher Power Algorithm

The reduced error state diagram still contains zero-cycles of period 1 and period 2. It can be modified to effectively eliminate the zero-cycles by introducing variable-length edges. For any state $s \in \mathcal{H}$, let $\mathcal{E}_s$ be the set of outgoing edges of s. A period-1 zero-cycle with edge sequence e_0 in $\mathcal{H}$ is modified as follows. The full label of each edge $f \in \mathcal{E}_{\boldsymbol{i}(e_0)}$ such that $f \neq e_0$ is changed to $(\mathcal{L}'_{\text{in}}(e_0))\mathcal{L}'_{\text{in}}(f)/\mathcal{L}'_{\text{out}}(f)$. Then the self-loop edge e_0 is removed from the diagram. A period-2 zero-cycle with edge sequence e_0e_1 is modified as follows. For each edge $e_i, i = 0, 1$, the following steps are taken.

1) The full edge label of each edge $f \in \mathcal{E}_{\boldsymbol{i}(e_i)}$ such that $f \neq e_i$ is changed to

$$(\mathcal{L}'_{\text{in}}(e_i)\mathcal{L}'_{\text{in}}(e_{i+1 \bmod 2}))\mathcal{L}'_{\text{in}}(f)/\mathcal{L}'_{\text{out}}(f).$$

2) For each edge $g \in \mathcal{E}_{\boldsymbol{t}(e_i)}$ such that $g \neq e_{i+1 \bmod 2}$, an edge h is added to the diagram. The initial state of the new edge is $\boldsymbol{i}(h) = \boldsymbol{i}(e_i)$ and the terminal state is $\boldsymbol{t}(h) = \boldsymbol{t}(g)$. This new edge is labeled

$$(\mathcal{L}'_{\text{in}}(e_i)\mathcal{L}'_{\text{in}}(e_{i+1 \bmod 2}))\mathcal{L}'_{\text{in}}(e_i)\mathcal{L}'_{\text{in}}(g)/\mathcal{L}'_{\text{out}}(g).$$

After this procedure, the edges e_0 and e_1 are removed from the diagram. The final diagram contains no zero-cycles, possibly an increase in the number of edges, and variable-length input labels. An example of the resulting modified reduced error state diagram is shown in Fig. 5, again for the PR2 channel.

The modified diagram represents the zero-cycles in a manner that allows a simple search for open and closed error events. The error event lists may be generated by a sequence of symbolic vector–matrix multiplications on the *symbolic adjacency matrix* $\mathrm{A}_{\mathcal{H}}$ [5, p. 65]. The entry $\mathrm{A}_{\mathcal{H}}(I, J)$ contains the formal sum of the labels of all edges from I to J, or a null symbol $\emptyset$ if there are no such edges. The matrices are multiplied using concatenation of error sequences. The multiplication is not commutative, and the null symbol $\emptyset$ satisfies $\emptyset\varepsilon_x = \varepsilon_x\emptyset = \emptyset$. The matrix corresponding to Fig. 5 is given by

$$\mathrm{A}_{\mathcal{H}} = \begin{bmatrix} + & 0 & \emptyset & \emptyset & \emptyset \\ \emptyset & -,+ & \emptyset & \emptyset & 0 \\ (-)+ & (-)0 & \emptyset & \emptyset & \emptyset \\ + & 0 & - & \emptyset & \emptyset \\ \emptyset & \emptyset & \emptyset & (0)+,(0)- & \emptyset \end{bmatrix}.$$

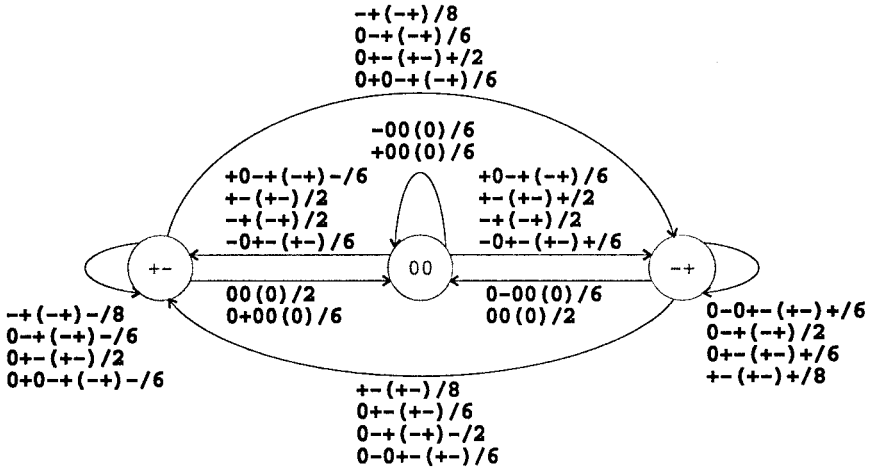

Fig. 4. The graph $\mathcal{F}$ for the PR2 channel, $h(D) = (1 + D)^2$, showing error fragments that accumulate no more than squared distance 8.

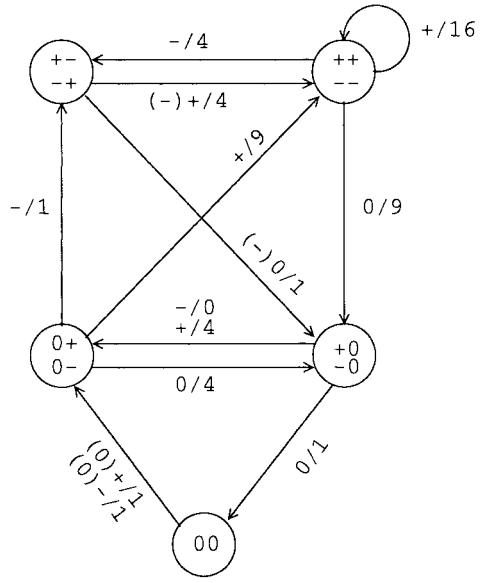

Fig. 5. Modified reduced error state diagram for the PR2 channel, $h(D) = (1 + D)^2$.

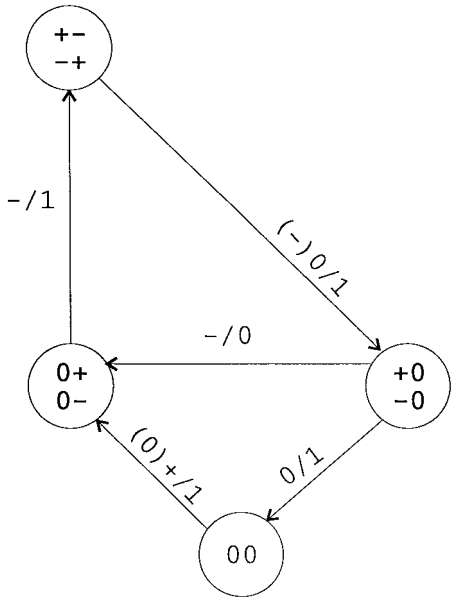

Fig. 6. Modified diagram showing required search depth for PR2 channel, $h(D) = (1 + D)^2$.

The start of an error event is denoted by the first nonzero label on a path starting at the zero-state. Closed and open error events at depth n are listed in $[\mathrm{A}_{\mathcal{H}}]^n((00),(00))$, and $[\mathrm{A}_{\mathcal{H}}]^n((00),(+-))$, respectively. For generating only simple error events, sequences returning to the zero-state are deleted from $\mathrm{A}_{\mathcal{H}}^{n-1}$ such that $\mathrm{A}_{\mathcal{H}}^{n} = \mathrm{A}_{\mathcal{H}}^{n-1}\mathrm{A}_{\mathcal{H}}$ contains no compound events. Parallel calculations are made for the squared distance, and paths that have accumulated distance greater than $d_{\max}^2$ may also be deleted from $\mathrm{A}_{\mathcal{H}}^{n-1}$.

For the symbolic matrix generation of events, it is necessary to have a method of determining when the search has completed. The search may simply terminate when all entries in the matrix $\mathrm{A}_{\mathcal{H}}^{n}$ have accumulated distance greater than $d_{\max}^2$. The exact number of matrix multiplications required is a function of the longest path in the diagram with distance less than or equal to $d_{\max}^2$. This search depth can be determined by pruning paths from the error state diagram (or a modified form of the error state diagram) as follows. For any path $f_1, \cdots, f_m$, if there exists a path $e_1, \cdots, e_n$ with $\boldsymbol{i}(e_1) = \boldsymbol{i}(f_1), \boldsymbol{t}(e_n) = \boldsymbol{t}(f_m)$ such that

$$\sum_{k=1}^{n} \mathcal{L}_{out}(e_k) = \sum_{k=1}^{m} \mathcal{L}_{out}(f_k)$$

and $n \geq m$ then remove the path $f_1, \cdots, f_m$ from the diagram, since there is a longer path that accumulates the same distance. Removing the path for $m = 1$ corresponds to removing an edge from the diagram, while longer paths may require graph manipulations to isolate the path of interest. The result of applying the construction to Fig. 5 is illustrated in Fig. 6. By examination of Fig. 6 one can show the number of matrix multiplications required to list all closed events of distance $d_{\max}^2$ is $\frac{3}{2}\ d_{\max}^2 - 2$ and the number required to list all open events also is $\frac{3}{2}\ d_{\max}^2 - 2$.

IV. Error Event Lists

Tables I and II list open and closed error events for a number of binary input partial-response channels. The lists contain all the

TABLE I
OPEN ERROR EVENTS FOR CHANNELS $h(D) = (1 - D)^m(1 + D)^n$

m	n	$\varepsilon_x(D)/\|\|\varepsilon_x(D)h(D)\|\|^2$	
0	1	+(-+)/1	+(-+)+(-+)+-(+-)-(+-)/13
		+(-+)+(-+)/5	+(-+)+-(+-)-(+-)-(+-)/13
		+-(+-)-(+-)/5	+-(+-)-(+-)-(+-)-(+-)/13
		+(-+)+(-+)+(-+)/9	+-(+-)-+(-+)+(-+)+(-+)/13
		+(-+)+-(+-)-(+-)/9	+(-+)+-(+-)-+(-+)+(-+)/13
		+-(+-)-(+-)-(+-)/9	+-(+-)-(+-)-+(-+)+(-+)/13
		+-(+-)-+(-+)+(-+)/9	+-(+-)-+(-+)+-(+-)-(+-)/13
		+(-+)+(-+)+(-+)+(-+)/13	
1	0	+(+)/1	+(+)-(-)+(+)-(-)+(+)-(-)/21
		+(+)-(-)/5	+(+)-(-)+(+)-(-)+(+)-(-)+(+)/25
		+(+)-(-)+(+)/9	+(+)-(-)+(+)-(-)+(+)-(-)+(+)-(-)/29
		+(+)-(-)+(+)-(-)/13	+(+)-(-)+(+)-(-)+(+)-(-)+(+)-(-)+(+)/33
		+(+)-(-)+(+)-(-)+(+)/17	+(+)-(-)+(+)-(-)+(+)-(-)+(+)-(-)+(+)-(-)/37
0	2	+-(+-)/2	+0-+(-+)0-+(-+)/8
		+-(+-)0+-(+-)/4	+-+(-+)0-0+-(+-)/8
		+-+(-+)0-+(-+)/4	+0-+-(+-)0+-(+-)/8
		+0-+(-+)/6	+-(+-)0+-(+-)0+-(+-)0+-(+-)/8
		+-(+-)0+-(+-)0+-(+-)/6	+-(+-)0+-(+-)0+-+(-+)0-+(-+)/8
		+-(+-)0+-+(-+)0-+(-+)/6	+-(+-)0+-+(-+)0-+(-+)0-+(-+)/8
		+-+(-+)0-+(-+)0-+(-+)/6	+-+(-+)0-+(-+)0-+(-+)0-+(-+)/8
		+-+(-+)0-+-(+-)0+-(+-)/6	+-+(-+)0-+-(+-)0+-(+-)0+-(+-)/8
		+-(+-)0-+(-+)/8	+-(+-)0+-+(-+)0-+-(+-)0+-(+-)/8
		+-+(-+)0+-(+-)/8	+-+(-+)0-+(-+)0-+-(+-)0+-(+-)/8
		+-(+-)0+0-+(-+)/8	+-+(-+)0-+-(+-)0+-+(-+)0-+(-+)/8
1	1	+(0+)/1	+(0+)-+(-+)0+(0+)-(+-)/4
		+(0+)+(+)/2	+0(+0)-(0-)/5
		+(0+)-(+-)/2	+(0+)+(+)0+(0+)+(+)0(+0)/5
		+(0+)+(+)0(+0)/3	+(0+)+(+)0+(0+)-(+-)0(-0)/5
		+(0+)-(+-)0(-0)/3	+(0+)-(+-)0-(0-)-(-)0(-0)/5
		+(0+)-+(-+)0(+0)/3	+(0+)-+(-+)0+(0+)+(+)0(+0)/5
		+(0+)+(+)0+(0+)+(+)/4	+(0+)+(+)0+(0+)-+(-+)0(+0)/5
		+(0+)+(+)0+(0+)-(+-)/4	+(0+)-(+-)0-(0-)+(-+)0(+0)/5
		+(0+)-(+-)0-(0-)-(-)/4	+(0+)-+(-+)0+(0+)-(+-)0(-0)/5
		+(0+)-(+-)0-(0-)+(-+)/4	+(0+)-(+-)0-(0-)+-(+-)0(-0)/5
		+(0+)-+(-+)0+(0+)+(+)/4	+(0+)-+(-+)0+(0+)-+(-+)0(+0)/5
1	2	+0(+0)/2	+-+-(+-)0-(0-)/4
		+-+(-+)/2	+0+(0+)+0+(0+)/4
		+0+(0+)++(+)/4	+-+(-+)00+0(+0)/4
		+0(+0)0+0(+0)/4	+-+(-+)00+-+(-+)/4
		+-+(-+)0+(0+)/4	+-+-(+-)00-0(-0)/4
		+0+(0+)-+(-+)/4	+-+-(+-)00-+-(+-)/4
		+0(+0)0+-+(-+)/4	
1	3	+-+-(+-)/4	+-+00+00+0+(0+)/8
		+0+(0+)/6	+-+00+00+-+-(+-)/8
		+-+00+0+(0+)/6	+-+00+-+00+0+(0+)/8
		+-+00+-+-(+-)/6	+-+-(+-)00-0-(0-)/8
		+-+0+0(+0)/8	+-+00+-+00+-+-(+-)/8
		+00+0+(0+)/8	+-+-(+-)00-+-+(-+)/8
		+00+-+-(+-)/8	+-+-+(-+)00+0+(0+)/8
		+-+0-+-+(-+)/8	+-+-+(-+)00+-+-(+-)/8
		+-+000+-+-(+-)/8	

TABLE II
CLOSED ERROR EVENTS FOR CHANNELS $h(D) = (1 - D)^m(1 + D)^n$

m	n	$\varepsilon_x(D)/\|\|\varepsilon_x(D)h(D)\|\|^2$	
0	1	+(-+)0/2	+-(+-)-(+-)-(+-)0/10
		+-(+-)0/2	+(-+)+-(+-)-(+-)0/10
		+(-+)+(-+)0/6	+(-+)+(-+)+-(+-)0/10
		+-(+-)-(+-)0/6	+-(+-)-(+-)-+(-+)0/10
		+(-+)+-(+-)0/6	+(-+)+-(+-)-+(-+)0/10
		+-(+-)-+(-+)0/6	+-(+-)-+(-+)+(-+)0/10
		+(-+)+(-+)+(-+)0/10	+-(+-)-+(-+)+-(+-)0/10
1	0	+(+)0/2	+(+)-(-)+(+)-(-)+(+)-(-)0/22
		+(+)-(-)0/6	+(+)-(-)+(+)-(-)+(+)-(-)+(+)0/26
		+(+)-(-)+(+)0/10	+(+)-(-)+(+)-(-)+(+)-(-)+(+)-(-)0/30
		+(+)-(-)+(+)-(-)0/14	+(+)-(-)+(+)-(-)+(+)-(-)+(+)-(-)+(+)0/34
		+(+)-(-)+(+)-(-)+(+)0/18	
0	2	+-(+-)00/4	+0-+-(+-)00/8
		+-+(-+)00/4	+-(+-)0+-(+-)0+-(+-)00/8
		+00/6	+-(+-)0+-(+-)0+-+(-+)00/8
		+-(+-)0+-(+-)00/6	+-(+-)0+-+(-+)0-+(-+)00/8
		+-(+-)0+-+(-+)00/6	+-+(-+)0-+(-+)0-+(-+)00/8
		+-+(-+)0-+(-+)00/6	+-+(-+)0-+-(+-)0+-(+-)00/8
		+-+(-+)0-+-(+-)00/6	+-(+-)0+-+(-+)0-+-(+-)00/8
		+-(+-)0+00/8	+-+(-+)0-+(-+)0-+-(+-)00/8
		+0-+(-+)00/8	+-+(-+)0-+-(+-)0+-+(-+)00/8
		+-+(-+)0-00/8	
1	1	+0(+0)0/2	+(0+)-(+-)0-(0-)-(-)0(-0)0/6
		+(0+)+(+)0(+0)0/4	+(0+)-+(-+)0+(0+)+(+)0(+0)0/6
		+(0+)-(+-)0(-0)0/4	+(0+)+(+)0+(0+)-+(-+)0(+0)0/6
		+(0+)-+(-+)0(+0)0/4	+(0+)-(+-)0-(0-)+(-+)0(+0)0/6
		+0(+0)-0(-0)0/6	+(0+)-+(-+)0+(0+)-(+-)0(-0)0/6
		+(0+)+(+)0+(0+)+(+)0(+0)0/6	+(0+)-(+-)0-(0-)+-(+-)0(-0)0/6
		+(0+)+(+)0+(0+)-(+-)0(-0)0/6	+(0+)-+(-+)0+(0+)-+(-+)0(+0)0/6
1	2	+0(+0)00/4	+0+(0+)+0+0(+0)00/6
		+-+(-+)000/4	+0+(0+)-+-(+-)000/6
		+-+-(+-)000/4	+-+-(+-)0-0(-0)00/6
		+-000/6	+0(+0)0+-+-(+-)000/6
		+0(+0)0+0(+0)00/6	+-+-(+-)00-0(-0)00/6
		+-+(-+)0+0(+0)00/6	+-+(-+)00+-+(-+)000/6
		+0+(0+)-+(-+)000/6	+-+(-+)00+-+-(+-)000/6
		+-+(-+)00+0(+0)00/6	+-+-(+-)00-+-(+-)000/6
		+0(+0)0+-+(-+)000/6	+-+-(+-)00-+-+(-+)000/6
1	3	+-+0000/6	+-+000+-+0000/10
		+-+00+-+0000/8	+-+00+00+-+0000/10
		+-+-(+-)0000/8	+-+00+-+00+-+0000/10
		+-+-+(-+)0000/8	+-+00+-+-(+-)0000/10
		+0000/10	+-+-(+-)00-+-0000/10
		+-+00+0000/10	+-+00+-+-+(-+)0000/10
		+00+-+0000/10	+-+-+(-+)00+-+0000/10
		+-+0-+-0000/10	

error events at distances less than or equal to the maximum distance listed for each channel. All error events have a corresponding symmetrical event, $\|h(D)\varepsilon_x(D)\|^2 = \|h(D)(-\varepsilon_x(D))\|^2$. Only one representative of the set $\{\pm\varepsilon_x(D)\}$ is listed in the tables.

V. CONCLUSIONS

Two algorithms for characterizing error events on partial-response channels have been presented. Lists of low-distance open and closed error events for binary input partial-response channels found in magnetic and optical recording applications were provided. The lists can be used to develop coding techniques to improve noise immunity on these channels [3], [11], [10], [8], [4], [7]. The lists can also be used to obtain the first few terms of the generating function for these channels [13].

REFERENCES

[1] S. A. Altekar, M. Berggren, B. E. Moision, P. H. Siegel, and J. K. Wolf, "Error-event characterization on partial-response channels," in *Proc. 1997 IEEE Int. Symp. Information Theory* (Ulm, Germany, 1997), p. 461.

[2] M. Berggren, "An algorithm for characterizing error event sequences in partial response channels," Diploma Project, Swiss Fed. Inst. Tech., Zurich, Switzerland, Aug. 1996.
[3] R. Karabed and P. H. Siegel, "Coding for higher-order partial-response channels," in *Coding and Signal Processing for Information Storage*, M. R. Raghuveer, S. A. Dianat, S. W. McLaughlin, and M. Hassner, Eds., *Proc. SPIE 2605*, Oct. 1995, pp. 115–126.
[4] R. Karabed, P. H. Siegel, and E. Soljanin, "Constrained coding for binary channels with high intersymbol interference," submitted for publication to *IEEE Trans. Inform. Theory*.
[5] D. Lind and B. H. Marcus, *An Introduction to Symbolic Dynamics and Coding*. Cambridge, U.K.: Cambridge Univ. Press, 1995.
[6] B. H. Marcus, P. H. Siegel, and J. K. Wolf, "Finite-state modulation codes for data storage," *IEEE J. Select. Areas Commun.*, vol. 10, pp. 5–37, Jan. 1992.
[7] B. E. Moision, P. H. Siegel, and E. Soljanin, "Distance-enhancing codes for digital recording," *IEEE Trans. Magn.*, vol. 34, no. 1, pt. 1, pp. 69–74, Jan. 1998.
[8] J. Moon and B. Brickner, "Maximum transition run codes for data storage systems," *IEEE Trans. Magn.*, vol. 32, pp. 3992–3994, Sept. 1996.
[9] W.-H. Sheen and G. L. Stuber, "Error probability for reduced-state sequence estimation," *IEEE J. Select. Areas Commun.*, vol. 10, pp. 571–578, Apr. 1992.
[10] P. H. Siegel "Coded modulation for binary partial response channels: state-of-the-art," in *Proc. 1996 Information Theory Workshop* (Haifa, Israel, June 9–13, 1996).
[11] E. Soljanin, "On coding for binary partial-response channels that don't achieve the matched-filter-bound," in *Proc. 1996 Information Theory Workshop* (Haifa, Israel, June 9–13, 1996).
[12] A. J. Viterbi and J. K. Omura, *Principles of Digital Communication and Coding*. New York: McGraw-Hill, 1979.
[13] A. D. Weathers, S. A. Altekar, and J. K. Wolf, "Distance spectra for PRML channels," *IEEE Trans. Magn.*, vol. 33, no. 5, pt. 1, pp. 2809–2811, Sept. 1997.

On the Distance Distribution of Duals of BCH Codes

Ilia Krasikov and Simon Litsyn, *Member, IEEE*

***Abstract*—We derive upper bounds on the components of the distance distribution of duals of BCH codes.**

***Index Terms*—BCH codes, distance distribution.**

I. Introduction

Let C be the code dual to the extended t-error correcting Bose-Chaudhuri–Hocquenghem (BCH) code of length $q = 2^m$, and let $B = (B_0, \cdots, B_q)$ stand for the distance distribution of C. Our aim is to derive *upper bounds* on B_i's. The following theorems summarize our present knowledge.

The first one shows that outside a certain interval B_i's vanish. This is a refinement of the celebrated result by Weil [18] and Carlitz–Uchiyama [3] due to Serre [14] (it has been adapted for duals of BCH codes in [6] and [12]).

Theorem 1: If $|q/2 - i| > 2(t-1)[2 \cdot 2^{m/2}]$, $i \neq 0, q$, then $B_i = 0$. □

The next result deals with divisibility properties and is based on the Ax theorem [2], see [7], [11], [13], and [16].

Theorem 2: Let a be the smallest positive integer $\geq m/[\log_2 2t]$. If i is not a multiple of 2^a then $B_{q/2-i} = 0$. □

Apart from some particular cases, namely $t = 1, 2, 3$, when all the values of the distribution were computed explicitly, to the extent of our knowledge, no general estimates of B_i's were published.

In this correspondence we derive upper bounds on B_i's. Roughly speaking, these bounds show that the distance distribution can be upper-bounded by the corresponding normal distribution. To derive the bounds we use the linear programming approach along with some estimates on the magnitude of Krawtchouk polynomials of fixed degree in a vicinity of $q/2$.

II. Preliminaries

Let $F = \boldsymbol{F}_q$ be the finite field of $q = 2^m$ elements and Tr denote the trace function from F to $\boldsymbol{F}_2$. Let $\mathcal{G}_t$ be an additive subgroup of $F[x]$

$$\mathcal{G}_t = \left\{ G(x) = \sum_{i=1}^{t} a_i x^{2i-1} : \quad a_i \in F \right\}.$$

Let α be a primitive element in F. For every $G(x) \in \mathcal{G}_t$ and $\epsilon \in \boldsymbol{F}_2$ we define a vector in $\boldsymbol{F}_2^q$

$$\boldsymbol{c}(G, \epsilon) = (\mathrm{Tr}\,(G(0)) + \epsilon, \mathrm{Tr}\,(G(1)) + \epsilon, \mathrm{Tr}\,(G(\alpha)) + \epsilon, \cdots, \mathrm{Tr}\,(G(\alpha^{q-2})) + \epsilon).$$

When $G(x)$ runs over $\mathcal{G}_t$, the set of vectors $\boldsymbol{c}(G, \varepsilon)$ constitute the code dual to the extended BCH codes of length q and with minimum distance $2t + 2$, see, e.g., [1], [10], and [15]. Let $w(\boldsymbol{c}(G, \epsilon))$ stand for the number of nonzero coordinates in $\boldsymbol{c}(G, \epsilon)$. For $i \in [0, q]$

$$B_i = |\{G(x) \in \mathcal{G}_t, \epsilon \in \boldsymbol{F}_2 : w(\boldsymbol{c}(G, \epsilon)) = i\}|.$$

It is easy to check that $B_0 = 1$ and $\sum_{i=0}^{q} B_i = 2|\mathcal{G}_t| = 2q^t$. By the MacWilliams identity

$$\sum_{j=0}^{q} B_j P_i(j) = \begin{cases} 2q^t, & i = 0 \\ 0, & 1 \leq i < 2t+2. \end{cases} \tag{1}$$

Here $P_i(j)$ are Krawtchouk polynomials (orthogonal on the interval $[0, q]$ with weight $\binom{q}{j}$) defined by the following recurrence (for their properties see, e.g., [5], and [8]–[10]):

$$(k+1)P_{k+1}(x) = (q-2x)P_k(x) - (q-k+1)P_{k-1}(x) \tag{2}$$
$$P_0(x) = 1 \qquad P_1(x) = q - 2x.$$

We need the following facts about Krawtchouk polynomials:

Orthogonality Relation:

$$\sum_{i=0}^{q} \binom{q}{i} P_\ell(i) P_k(i) = \delta_{\ell,k} 2^q \binom{q}{\ell}.$$

Manuscript received November 24, 1997; revised July 16, 1998.

I. Krasikov is with the School of Mathematical Sciences, Tel-Aviv University, Ramat-Aviv 69978, Tel-Aviv, Israel. He is also with the Beit-Berl College, Kfar-Sava, Israel.

S. Litsyn is with the Center for Discrete Mathematics, Rutgers University, Piscataway, NJ 08854 USA, on leave from the Department of Electrical Engineering–Systems, Tel-Aviv University, Ramat-Aviv 69978, Tel-Aviv, Israel (e-mail: litsyn@eng.tau.ac.il).

Communicated by A. Barg, Associate Editor for Coding Theory.
Publisher Item Identifier S 0018-9448(99)00083-8.